PRAMANA
— journal of
physics

Vol. 60, No. 3
March 2003
pp. 535–546

Non-equilibrium and band tailing in organic conductors

A T OZA*, P C VINODKUMAR and R G PATEL
Department of Physics, Sardar Patel University, Vallabh Vidyanagar 388 120, India
*Email: headphys@spu.ernet.in

MS received 22 October 2001; revised 29 April 2002; accepted 21 August 2002

Abstract. The concept of band tailing with focal point and width of the tail from IR absorption spectra of different organic conductors is found valid even for thermal and elastic changes. The experimental situations like change of solvents, method of preparation, applied pressure and pressure cycle apart from compositions is analyzed within the framework of tailing of states. Non-equilibrium due to coupling between applied energy and free electrons can be responsible for the exponential relaxation from non-equilibrium to equilibrium.

Keywords. Band tailing; organic conductors; IR spectra; electrical resistivity.

PACS Nos 78.30.Jw; 72.80.Le; 72.90.+y

1. Introduction

Study of organic conductors and semiconductors continues to generate interest with the report of completely new materials possessing novel features [1–4]. Many inclusion and charge transfer organic complexes were studied both experimentally and theoretically under different conditions like temperature and pressure [5–8]. The IR absorption properties of donor–acceptor complexes of organo-metallic chelates have been studied [9,10]. It has already been known that the organic semiconductors can also be treated like the conventional semiconductors but with partially stabilized conduction bands [11–18].

In semiconductors, the absorption coefficient falls exponentially near the optical absorption edge [19]. The tail states can be either within the conduction or valence band or extending within the forbidden energy gap. This so called Urbach tail is of the order of thermal energy for ordered materials [20]. Band tailing reduces band gap or the activation energy and increases conductivity. For disordered materials, the width of the tail can be much larger than the thermal energy. Here we analyze the experimental results of benzidine–iodine, benzidine–DDQ, benzidine–TCNQ and amylose–iodine complexes. A schematic description of the band structure of iodine complexes and a representation of direct and indirect band structures are shown in figure 1. It is interesting to note that the straight lines of the semilog plot of absorption coefficient (α); i.e., log α vs. $h\nu$ meet at a common point for various compositions [21,22]. This common point, we refer here as the focal point. Similar focal points are observed in the cases of log R vs. $K_{\mathrm{B}}T$ as well as

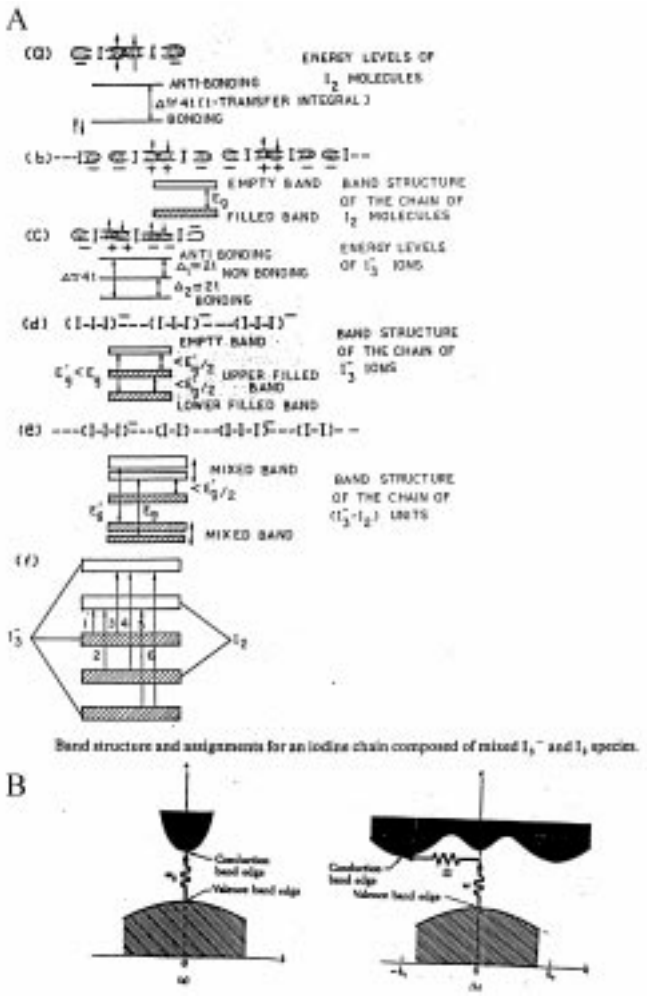

Band structure and assignments for an iodine chain composed of mixed I_3^- and I_2 species.

Figure 1. Schematic description of the band structure (**A**) and direct–indirect band structure (**B**) of charge transfer complexes.

log R vs. E_{el} (elastic energy $\propto P^2$) (see figures 2–4). The distinct linear behavior with focal points seen here suggests us to explore and understand the physical meaning of the same.

Different materials are studied experimentally for electrical conductivity with temperature as well as with elastic energy supplied through external pressure. From the different material samples with varying compositions we infer that this focal point would be a generic character of the material.

Here the cases related to ln α vs. $h\nu$ plot is generalized for the similar behavior observed in log R vs. $K_{\mathrm{B}}T$ and log R vs. (pressure)^2 plots. It is also seen that not only compositions lead to different widths of the tail but it also depends on the type of solvents for preparation, method of preparation, variation in the way the pressures are applied etc. They also lead to similar tailing effects.

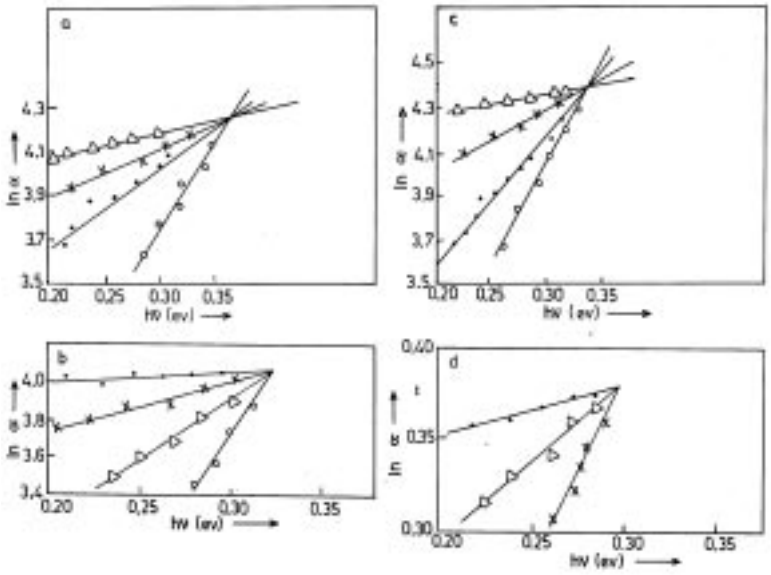

Figure 2. In α vs. $h\nu$ plots of various charge transfer complexes like benzidine–iodine with different compositions (**a**), with different solvents (**b**), benzidine–DDQ (2:3) prepared using various solvents (**c**), and amylose–iodine prepared using different methods (**d**).

This paper is an attempt to understand and explain the common characteristics of the focal points seen experimentally on amylose–iodine, benzidine–iodine, benzidine–DDQ and benzidine–TCNQ complexes under different situations.

2. Experimental details

A detailed account of the compound preparations of these complexes can be found in literature [23–26]. However, a brief resume of their preparation would be appropriate here, as that is relevant to the present analysis.

Four compositions of benzidine–iodine complexes were prepared from chloroform [23]. Benzidine–DDQ (DDQ=2,3-dichloro-5,6-dicyano-p-benzoquinone) always formed 2:3 stoichiometric complex [24]. Benzidine–DDQ was prepared from chloroform, carbon tetrachloride, nitrobenzene, dimethyl formamide and tetrahydrofuran. Benzidine–TCNQ (TCNQ=7,7,8,8-tetracyano-p-quino-dimethane) was prepared from dichloromethane. Chloroform and carbon tetrachloride are non-polar solvents and nitrobenzene, dimethyl formamide and tetrahydrofuran are polar solvents.

Disordered types of amylose–iodine were prepared by three different methods [25]. Amylose–iodine (type-I) was prepared as thick blue films or flakes by complete evaporation of an intense blue solution heated above gelatization temperature before the addition of KI–I_2 solution in water. Type-II samples were prepared from the precipitates of the complex from a hot solution using precipitating agents like potassium dichromate. Samples were washed with hot water to remove the precipitating agent before measurements. Type-III samples were prepared by directly staining amylose gains with iodine.

Low temperature measurements for the electrical conductivity were carried out using continuous flow cryostat [26]. High-pressure measurements for the electrical conductivity were performed using Bridgman anvil apparatus [27,28]. The Nujol mull transmission spectra in the range of 400–4000 cm^{-1} were obtained experimentally for the measurements involving infrared absorption using a standard spectro-photometer of Unicam Company.

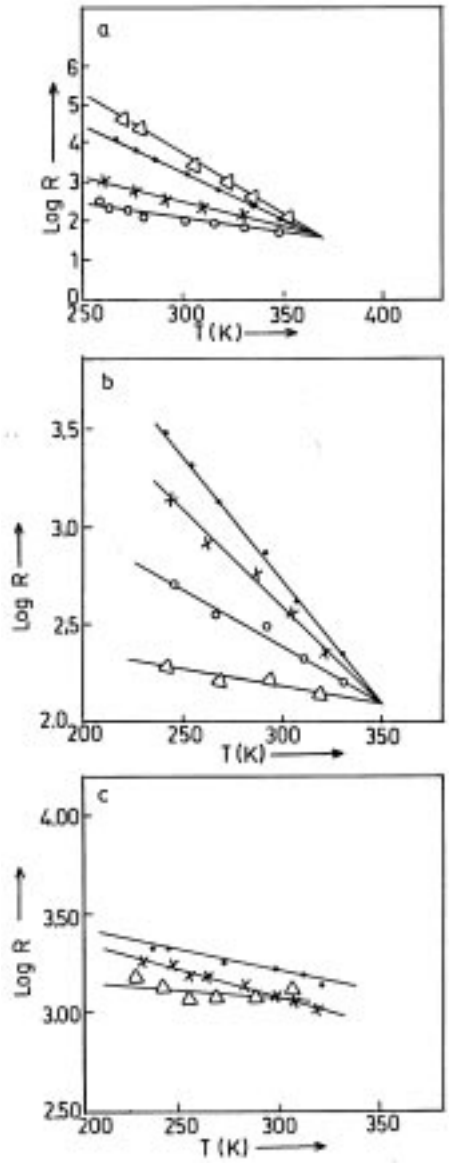

Figure 3. Log R vs. T (K) plots of benzidine–iodine with various compositions (**a**), benzidine–iodine prepared using various solvents (**b**) and benzidine–TCNQ at different pressures (**c**).

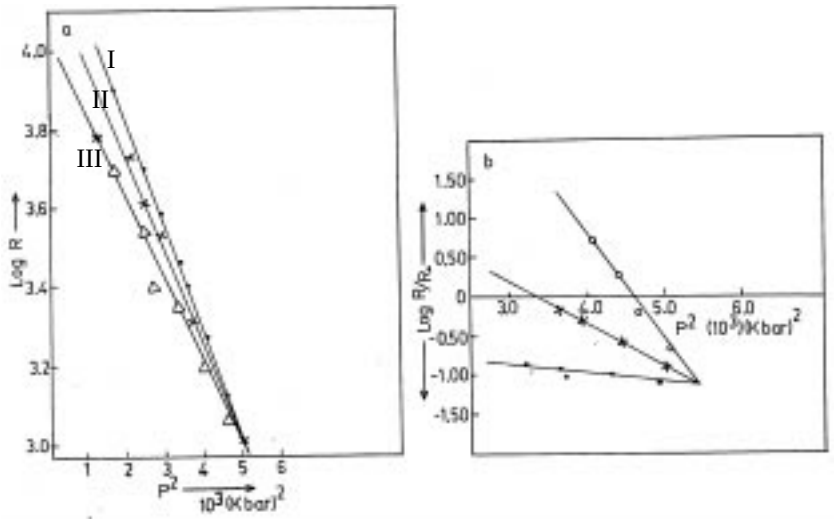

Figure 4. Log R vs. P^2 (work done by pressure) for various runs of the same sample of benzidine–TCNQ (**a**) various runs are marked I, II, III respectively and $\log(R/R_0)$ vs. P^2 (work done by pressure) of amylose–iodine prepared by different methods (**b**).

3. Results and observations

From the experimental data for the infrared absorption coefficients (α), $\ln\alpha$ vs. $h\nu$ is plotted for various compositions of benzidine–iodine (figure 2a). Here the variation in $\ln\alpha$ is considerably suppressed due to weak ionic bonding and strong electron–phonon interactions. So, α does not vary by several orders of magnitude. $E_1 = 0.36$ eV is the common point for all compositions. The width of the tail (E_0) vs. compositions is also plotted in figure 5. Here the variation in $\ln\alpha$ is less than that in the case of GaAs, as expected for the disordered materials. Also the exponential function becomes constant for large values of independent variable and it depends on range considered.

The $\ln\alpha$ vs. $h\nu$ plot for benzidine–iodine (2:3) prepared from chloroform, carbon tetrachloride, DMF (di-methyl formamide), and nitrobenzene is plotted and is found to furnish similar variation in the width of the tail (figure 2b) with $E_1 = 0.32$ eV.

Benzidine–DDQ exists in 2:3 stoichiometric form and is prepared from various solvents. The $\ln\alpha$ vs. $h\nu$ is plotted (figure 2c) and the widths that relate to the slopes of the straight lines, and their focal point (0.33 eV) are found. The variation of α is less here because of ionic bonding.

Amylose–iodine has an optical absorption edge near 0.44 eV and below this edge, $\ln\alpha$ vs. $h\nu$ is plotted for this inclusion compound prepared by various methods (figure 2d). Even different methods of preparation lead to a variation in the width of exponential relaxation. Ionic bonding leads to a little variation in α rather than by several orders of magnitude.

When the various compositions of benzidine–iodine were studied, it was found that there was a deviation from straight line in $\log R$ vs. $1000/T$ plots near the temperature of crossing among various compositions. Therefore, $\log R$ vs. T was plotted which indeed regulated into a crossing of lines for four compositions at a common point (figure 3a).

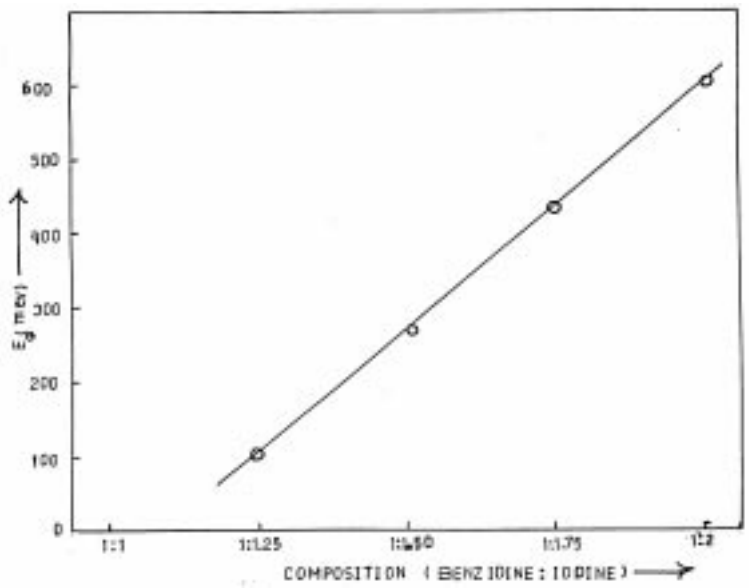

Figure 5. Width of band tail vs. composition for benzidine–iodine.

Polar solvents create more disordered lattice compared to a non-polar solvent revealing large widths of relaxation. Molecules of polar solvents go into the lattice and form inclusion complexes. For different solvents, similar effect was found in the case of benzidine–iodine (2:3) (figure 3b).

The temperature dependence of resistivity of benzidine–TCNQ was studied at different pressures. Pressure, like the radiation introduces non-equilibrium with respect to filling of the density of states. A direct band gap semiconductor becomes an indirect band gap semiconductor involving absorption of phonon. This is well known for semiconductors under high pressure. It is because there is a movement of valley in the band structure when pressure is applied. Log R vs. T at different pressure is plotted for benzidine–TCNQ (figure 3c).

Other ways to generate change in the width of relaxation would be through elastic energy introduced by applying pressures. A case study of the effect of pressure cycles for benzidine–TCNQ is used here. High-pressure runs were made on the same sample and curves of various runs were also found to meet at a common point. This involves history of compression. Effects of an earlier or previous run remains (figure 4a).

Amylose–iodine samples prepared by three different methods were also studied under high pressures. Curves of at least three types of samples were found to meet at common point (figure 4b).

Benzidine–iodine was found to show an indirect transition with $E_g = 0.3$ eV and phonon energy, E_p of 0.03 eV. Considering the focal point (E_1) to be the Fermi-level in this heavily doped semiconductor, $E_1 = E_i = E_g + E_p + \xi_p$ where ξ_p is due to band filling effect or a Burstein–Moss shift parameter. The Fermi level lies in the conduction hand and ξ_p can be calculated from focal point. E_g and E_p are obtained from optical absorption edges (tables 1 and 2). From the data on resistivity with temperature, it was found $E_1 = E_g + E_p$ only,

as temperature affects the phonon spectrum and there is strong electron–phonon interaction. The focal points at $E_1 = 0.037$ eV and $E_1 = 0.032$ eV were found with variation in compositions (table 3) and with variations in solvents (table 4) respectively.

Ln α vs. $h\nu$ for benzidine–DDQ (2:3) prepared from various solvents also leads to the estimation of ξ_p (table 5). For amylose–iodine prepared by various methods lead to $E_1 = 0.45$ eV with $\xi_p = 0$ (table 6) as there is no charge transfer in an inclusion compound. Only charge transfer leads to band filling and provide non-zero ξ_p.

Log R vs. T at different pressure for benzidine–TCNQ gives $E_1 = E_p = 0.031$ eV (table 7), since temperature variation affects only phonon spectrum.

Table 1. Width of tail from ln α vs. $h\nu$ for various compositions of benzidine–iodine.

Compositions	E_g (eV)	ξ_n (eV)	E_0 (meV)	E_1 (eV)
1:1.00	0.12	0.21	100	
1:1.50	0.03	0.30	270	
				0.36
1:1.75	0.01	0.32	430	
				$(E_g + E_p + \xi_n)$
1:2.00	0.20	0.13	600	

Table 2. Width of tail from ln α vs. $h\nu$ for various solvents of benzidine–iodine.

Solvents	E_g (eV)	ξ_n (eV)	E_0 (meV)	E_1 (eV)
CCl_4	0.12	0.18	60	
$CHCl_3$	0.10	0.20	156	
				0.325
$C_6H_5NO_2$	0.08	0.22	400	
				$(E_g + E_p + \xi_n)$
DMF	0.05	0.24	1800	

Table 3. Width of tail from ln R vs. $K_B T$ for various compositions of benzidine–iodine.

Compositions	E_0 (meV)	E_1 (eV)
1:1.00	22.07	
1:1.50	18.05	
1:1.75	9.03	0.037
		$E_g(0)$
1:2.00	6.77	

Table 4. Width of tail from ln R vs. $K_B T$ for various solvents of benzidine–iodine.

Solvents	E_g (meV)	E_1 (eV)
CCl_4	12.36	
$CHCl_3$	22.56	
		0.032
$C_6H_5NO_2$	39.48	
		$E_g(0)$
THF	124.08	

Table 5. Width of tail of benzidine–DDQ (2:3) from ln α vs. $h\nu$ plot for various solvents.

Solvents	E_g (eV)	ξ_p (eV)	E_0 (meV)	E_1 (eV)
CCl_4	0.25	0.06	40	
$CHCl_3$	0.23	0.08	148	
				0.34
$C_6H_5NO_2$	0.21	0.10	367	
				$(E_g + E_p + \xi_p)$
THF	0.29	0.12	1214	

Table 6. Widths of tail from ln α vs. $h\nu$ plot for amylose–iodine prepared by different methods.

Methods	E_g (eV)	ξ_p (eV)	E_0 (meV)	E_1 (eV)
I	0.44	0.01	400.0	
II	0.43	0.02	112.5	
				0.45
				$(E_g + E_p)$
III	0.40	0.05	50.0	

Table 7. Widths of tail from log R vs. K_BT plot for benzidine–TCNQ at different pressures.

Pressure in kilobars	E_g (eV)	E_0 (meV)	E_1 (eV)
44	0.24	67.68	
48	0.23	101.52	0.031
53	0.22	180.50	$E_g(0)$

4. Discussion and analysis

Although the organic charge transfer complexes are strongly correlated electron systems with σ and π orbital which are de-localized, the energy band structure and consequences of the bands can be inferred through the IR absorption studies. In the complexes studied here, there is charge transfer from donor to acceptor. Either the electron being transferred moves or the free charges in donor or acceptor stacks move in partially filled bands. Many effects of band structure like band tailing, Burstein–Moss shift, Franz–Keldysh effect, Redfield effect, direct and indirect transitions, free carrier absorption etc. were all discussed in organic semiconductors [11–18]. Under this premise, the band structure description is meaningful in the present analysis also.

For the complexes considered here, the Fermi level is taken to be in the parabolic portion of a band and therefore, the initial density of states is proportional to $E_v^{1/2}$ or $E_c^{1/2}$. As the density of final state at energy E, can be taken as $N_f = N_0 \exp(E/E_0)$, we can write for an external source of absorption energy $E_{\text{ext}} = h\nu$ and $|\xi_p| = |\xi_n| = \xi$,

$$\alpha(h\nu = E_{\text{ext}}) = A \int_{\xi}^{\xi + E_{\text{ext}}} |E_{v/c}|^{1/2} \exp\{(E + E_g + E_p)/E_0\} \mathrm{d}E. \quad (1)$$

Substituting $E_{v/c} = E + E_g + E_p - E_{\text{ext}}$ and making a change of variable,

$$X = \{E_{\text{ext}} - (E_g + E_p + E)\}/E_0 \tag{2}$$

so that

$$\alpha(E_{\text{ext}}) = -A\exp(E_{\text{ext}}/E_0)\int_{E_{\text{ext}}-(E_g+E_p+\xi))/E_0}^{(E_g+E_p+\xi)/E_0} X^{1/2}\exp(-X)\mathrm{d}X. \tag{3}$$

For compounds whose $E_g + E_p + \xi$ satisfy, $E_{\text{ext}} \gg E_g + E_p + \xi$ for the external source of energy for absorption, we can set the lower limit to infinity then the integral becomes,

$$\alpha(E_{\text{ext}}) = AE_0^{3/2}\exp(E_{\text{ext}}/E_0)\int_{(E_g+E_p+\xi)/E_0}^{\infty} X^{1/2}\exp(-X)\mathrm{d}X. \tag{4}$$

The integral is an incomplete gamma function and is given by

$$\alpha(E_{\text{ext}}) = AE_0^{3/2}\exp(E_{\text{ext}}/E_0)\Gamma(3/2,(E_g+E_p+\xi)/E_0). \tag{5}$$

Using the asymptotic limit for the incomplete gamma function [29,30] we can have

$$\alpha(E_{\text{ext}}) = AE_0^{3/2}E_1^{1/2}[\exp(E_{\text{ext}}-E_1)/E_0)]\left[+\frac{1/2}{E_1} + \frac{(1/2)(-1/2)}{E_1^2} + \cdots\right] \tag{6}$$

where $E_1 = E_g + E_p + \xi$.

While for compounds whose E_1 is of the order of the external energy E_{ext}, the lower integral limit can be set equal to zero. For such cases, eq. (3) becomes

$$\alpha(E_{\text{ext}}) = -AE_0^{3/2}E_1^{3/2}[\exp(E_{\text{ext}}-E_1)/E_0]\sum_{k=0}^{\infty}\frac{E_1^k}{3/2.5/2\cdots(3/2+k)}. \tag{7}$$

Here, the integral relation $\int_0^u x^{p-1}\exp(-x)\mathrm{d}x = \exp(-u)\sum_{k=0}^{\infty}u^{p+k}/[p(p+1)\ldots(p+k)]$ is being used [30]. For compounds of our interest here, E_1 is very small of the order of infrared range or $K_{\text{B}}T$. So eq. (7) can be approximated as

$$\alpha(E_{\text{ext}}) = \alpha_0\exp\left(\frac{E_{\text{ext}}-E_1}{E_0}\right). \tag{8}$$

For the absorption study of electro-magnetic radiation $E_{\text{ext}} = h\nu$, while in the case of thermal as well as the pressure studies E_{ext} is given by $K_{\text{B}}T$ and P^2 corresponds to elastic energy, respectively. For charge transfer complexes, $E_1 = E_g + E_p + \xi$ and for the inclusion compounds $E_1 = E_g + E_p$.

Equation (8) can also be extended for the analysis of the temperature variations of the resistance or the conductivity of the compounds presented here, as the conductivity σ is related to the absorption coefficient α as

$$\sigma = \frac{\alpha n_1 c}{4\pi}. \tag{9}$$

Here we assume a quasi-static situation for which α and σ have similar dependence of pressure and temperature. dc Conductivity and ac conductivity linearly scale with each

other. This assumption is valid because in a large number of complexes dc conductivity and optical conductivity scale with each other.

Therefore σ also follow similar exponential relation given by eq. (8). The refractive index n_1, though a function of frequency, can be considered a constant in the thermal as well as moderate elastic energy range studied in this paper. The thermal expansion and consequent dilation leads to a change in the forbidden energy gap E_g. For many semiconductors the empirical relation is given by

$$E_g(T) = E_g(0) - \frac{aT^2}{b+T} \tag{10}$$

where a and b are constants [31]. At temperatures much lower than the Debye temperature, the energy gap is proportional to the square of the temperature. Much above the Debye temperature, the energy gap varies linearly with temperature. For $b \ll T$,

$$E_g(T) = E_g(0) - aT \tag{11}$$

and therefore

$$\sigma = \sigma_0 \exp\left[\frac{aT}{K_B T_0} - \frac{E_g(0)}{K_B T_0}\right]$$

or

$$\rho = \rho_0 \exp\left[\frac{E_g(0)}{K_B T_0} - \frac{aT}{K_B T_0}\right]. \tag{12}$$

On comparing eqs (7) and (12) in the light of eq. (9), we can identify $E_1 = E_g(0)$ and represent it as $K_B T_1$.

For the thermal analysis, we consider the Boltzmann distribution,

$$n = n_0 \exp(-\varepsilon/K_B T). \tag{13}$$

With the anharmonic oscillator nature for the crystal potential due to thermal variation

$$U(x) = cx^2 - gx^3 - fx^4 \tag{14}$$

the thermal expansion which leads to an irreversible displacement is given as [32]

$$\langle x \rangle = \frac{3g}{4c^2} K_B T. \tag{15}$$

So substituting $\varepsilon = \varepsilon_0 - 1/2k\langle x\rangle^2$ in eq. (13), and as the conductivity σ is proportional to n, we get

$$\sigma = \sigma_0 \exp\left[\left(1/2k\left(\frac{3g}{4c^2}K_B T\right)^2 - \varepsilon_0\right) \Big/ K_B T\right]$$

or

$$\rho = \rho_0 \exp\left[\left(\varepsilon_0 - 2k\left(\frac{3g}{4c^2}K_B T\right)^2\right) \Big/ K_B T\right]. \tag{16}$$

Thus $\ln R$ vs. T gives a straight line near focal point. Comparing eqs (12) and (16) with eq. (9), it can be deduced that thermal expansion also lead to the band tailing effect.

Now in the case of pressure studies, the elastic energy is proportional to (pressure)^2 and this energy causes a change in the exchange interaction and broadens the valence band. This reduces the energy band gap as

$$E_g(P) = E_g(0) - \gamma P^2 \tag{17}$$

where γ is related to the elastic constant of the compound. Accordingly, we can write

$$\rho = \rho_0 \exp\left[\frac{(E_g(0) - \gamma P^2}{2K_B T}\right]. \tag{18}$$

On comparing with eq. (9), we can identify $E_g(0)$ with the focal point and is proportional to P_1^2.

In the case of thermal energy, thermal phonons are responsible for exponential tailing of free carrier states. There can be eventual coupling between electron and phonon generating a transient polaron. In the case of electro-magnetic energy, phonons involved in indirect transitions are coupled with free charge carriers. In the case of elastic energy under high pressure, a change from direct to indirect band gap involving creation of phonon by deformation is responsible for relaxation of free carrier energy states. There is a possibility of transient coupling between phonons and charge carriers and consequent creation of virtual polarons.

5. Conclusion

The concept of band tailing with focal point from absorption spectra is generalized for thermal and elastic effects in organic conductors. The same effects are observed with the change of solvents, methods of preparations, applied pressures and pressure cycles as in the case of variation in compositions. The results are analyzed based on transition between band tails. The non-equilibrium regarding filling of density of states leads to exponential relaxation. In this paper, we generalized the concept of band tailing with focal points and widths of the IR absorption spectra to the thermal and pressure variations of the charge transfer complexes.

References

[1] Y A Starodub, E M Hinzman, Yu A Kaftanara and J Olejniczak, *Theor. Exp. Chem.* (USA) **33**, 95 (1997)

[2] T J Savenge, E Moons, G K Boschloo, A Croscus and T J Schoolam, *Phys. Rev.* **B55**, 9685 (1997)

[3] H Tachibara, T Kawai, R M Metzger, Kyukuon Zong and M P Caver, *Synth. Metals* **84**, 429 (1997)

[4] R Wojerchowski, J Ulansf, M Krydjewski, A Traoz, J K Jeszna, H Mueller, S Lefrant and C Faulquous, *Synth. Metals* **94**, 27 (1998)

[5] A T Oza, *Phys. Status Solidi* **80**, 573 (1983)

[6] A T Oza, *Bull. Mater. Sci.* (India) **7**, 401 (1985)
[7] A T Oza and P C Vinodkumar, *Indian J. Phys.* **A72**, 171 (1998)
[8] A T Oza, *Indian J. Phys.* **A73**, 373 (1999)
[9] A T Oza, *Cryst. Res. Tech.* **20**, 991 (1985)
[10] R G Patel and A T Oza, *Indian J. Phys.* **B74**, 31 (2000)
[11] A T Oza, *Czech. J. Phys.* **B33**, 1148 (1983)
[12] A T Oza, *Mol. Cryst. Liq. Cryst.* **10**, 377 (1984)
[13] A T Oza, *Aust. J. Phys.* **42**, 203 (1989)
[14] A T Oza, *Solid State Commun.* **71**, 1005 (1989)
[15] A T Oza, *Bull. Ind. Ass. Phys. Teachers* **15**, 165 (1998)
[16] A T Oza, *Phys. News* **27**, 89 (1996)
[17] K D Patel and A T Oza, *Indian J. Phys.* **B71**, 161 (1997)
[18] A T Oza, *High Pressure Res.* **17**, 47 (2000)
[19] J I Pankove, *Optical process in semiconductors* (Prentice Hall Inc., 1971) p. 45
[20] F Urbach, *Phys. Rev.* **92**, 1324 (1953)
[21] J I Pankove, *Phys. Rev.* **A140**, 2059 (1965)
[22] T S Moss and T D F Hawkins, *Infrared Phys.* **1**, 111 (1961)
[23] A V Nalini, A T Oza, Kumar Anil and E S R Gopal, *Proc. Nucl. Solid State Phys. Symp.*, Ahmedabad, India, Dec. 27–31, **19C**, 41 (1976)
[24] A V Nalini, Ph.D. Thesis, Indian Institute of Science, Bangalore (1978)
[25] A T Oza, Ph.D. Thesis, Indian Institute of Science, Bangalore (1980)
[26] A T Oza, *Indian J. Cryogenics* **10**, 62 (1985)
[27] A T Oza, *Phys. Status Solidi* **B114**, K171 (1982)
[28] S V Subramanyam, *Proc. Solid State Symp.*, Tirupati, India, **C35**, 2 (1992)
[29] M Abramowitz and I A Segun, *Hand book of mathematical functions* (Dover Publishers, New York, 1968) p. 260
[30] I S Gradshteyn and I M Ryzhik, *Table of integral series and products* (Academic Press, New York, 1980) p. 317
[31] Y P Varshni, *Physica* **34**, 149 (1967)
[32] C Kittel, *Introduction to solid state physics* (John Wiley and Sons, New York, 1991) 6th Edn., p. 114